HHS Public Access

Author manuscript

Nanoscale. Author manuscript; available in PMC 2017 January 13.

Published in final edited form as:

Nanoscale. 2016 April 28; 8(17): 9390–9397. doi:10.1039/c6nr01136e.

Ultrasensitive fluorescence immunoassay for detection of ochratoxin A using catalase-mediated fluorescence quenching of CdTe QDs†

Xiaolin Huang[a], **Shengnan Zhan**[a], **Hengyi Xu**[a], **Xianwei Meng**[b], **Yonghua Xiong**[a], and **Xiaoyuan Chen**[c]

[a]State Key Laboratory of Food Science and Technology, Nanchang University, Nanchang 330047, P. R. China. yhxiongchen@163.com; Fax: +86-791-8833-3708; Tel: +86-791-8833-4578

[b]Laboratory of Controllable Preparation and Application of Nanomaterials, Center for Micro/nanomaterials and Technology, Technical Institute of Physics and Chemistry, Chinese Academy of Sciences, Beijing 100190, P. R. China

[c]Laboratory of Molecular Imaging and Nanomedicine (LOMIN), National Institute of Biomedical Imaging and Bioengineering (NIBIB), National Institutes of Health (NIH), Bethesda, Maryland 20892, USA. shawn.chen@nih.gov; Tel: 301-451-4246

Abstract

Herein, for the first time we report an improved competitive fluorescent enzyme linked immunosorbent assay (ELISA) for the ultrasensitive detection of ochratoxin A (OTA) by using hydrogen peroxide (H_2O_2)-induced fluorescence quenching of mercaptopropionic acid-modified CdTe quantum dots (QDs). In this immunoassay, catalase (CAT) was labeled with OTA as a competitive antigen to connect the fluorescence signals of the QDs with the concentration of the target. Through the combinatorial use of H_2O_2-induced fluorescence quenching of CdTe QDs as a fluorescence signal output and the ultrahigh catalytic activity of CAT to H_2O_2, our proposed method could be used to perform a dynamic linear detection of OTA ranging from 0.05 pg mL^{-1} to 10 pg mL^{-1}. The half maximal inhibitory concentration was 0.53 pg mL^{-1} and the limit of detection was 0.05 pg mL^{-1}. These values were approximately 283- and 300-folds lower than those of horseradish peroxidase (HRP)-based conventional ELISA, respectively. The reported method is accurate, highly reproducible, and specific against other mycotoxins in agricultural products as well. In summary, the developed fluorescence immunoassay based on H_2O_2-induced fluorescence quenching of CdTe QDs can be used for the rapid and highly sensitive detection of mycotoxins or haptens in food safety monitoring.

1. Introduction

Enzyme-linked immunosorbent assay (ELISA) is a simple, rapid, high-throughput, and cost-effective technique that has been considered as the most commonly used method to detect

†Electronic supplementary information (ESI) available. See DOI: 10.1039/c6nr01136e

Correspondence to: Yonghua Xiong; Xiaoyuan Chen.

harmful food-borne substances. However, the sensitivity of conventional ELISA ranges from ng mL^{-1} to μg mL^{-1}. In most cases, harmful food-borne substances are undetectable by using conventional ELISA because the concentrations of these substances are at the pg mL^{-1} level or even lower in food pollutants. Therefore, ultrasensitive immunoassays should be developed to detect harmful food-borne substances at low pg mL^{-1} levels.

Various improved immunoassays with ultrahigh sensitivity have been developed to detect target molecules.[1–9] Among these strategies, the introduction of novel signal generation transducers to convert molecular recognition events into detectable outputs has been widely used to enhance the detection sensitivity of conventional ELISA. Some of these techniques include fluorescent ELISA,[10] chemiluminescent ELISA,[11] electrochemical ELISA,[12] pH meter-based ELISA,[13] glucose meter-based ELISA,[14] volumetric ELISA,[15] Raman ELISA,[16] digital ELISA,[17] and plasmonic ELISA.[18] The use of fluorescence signals to replace absorbance is a simple and promising method; in this method, a relatively small amount of fluorescent molecules are required to generate a measurable fluorescence signal to increase the sensitivity of ELISA.[19–21] Nevertheless, traditional organic fluorophores are characterized by relatively low fluorescence intensity and are vulnerable to photobleaching[20,21] that can deteriorate the reproducibility of an immunoassay. To overcome these problems, researchers used luminescent nanomaterials with enhanced fluorescence and photostability as alternative labels for the signal output in fluoroimmunoassays.[22–24] Among these materials, quantum dots (QDs) are optimum fluorescent labels because of their broad excitation, narrow emission spectra, large Stokes shifts, and high photostability.[25,26] For example, Zhu *et al.* developed a fluoroimmunoassay for the highly sensitive detection of Cry1Ab protein by using antibody–QD conjugates as labels.[27] Zhang *et al.* also used antibody–QD conjugates as fluorescent reporters to develop a fluoroimmunoassay for the rapid and sensitive detection of aflatoxin B_1.[28] Nonetheless, immobilizing the antibody on the QD surface may result in inevitable loss of antibody activity because of its random orientation[29,30] that reduces the detection sensitivity. Moreover, the conditions for the purification of antibody–QD conjugates are pretty harsh due to their small size that limits their wide application in immunoassay.

Previous studies have demonstrated that the fluorescence intensity of mercaptopropionic acid (MPA) modified CdTe QDs can be efficiently quenched by low concentration hydrogen peroxide (H_2O_2) due to the detaching of thiolated molecules from the surface of QDs and the oxidation of tellurium in CdTe QDs.[31–34] According to the principle, many fluorescent biosensors have been developed for the sensitive detection of H_2O_2-related enzyme systems and their inhibitors.[35–39] However, to the best of our knowledge, a fluoroimmunoassay using only CdTe QDs as a fluorescent signal output instead of involving the immunological recognition has not yet been developed.

In this study, a novel fluorescent ELISA was developed by introducing H_2O_2-induced fluorescence quenching of CdTe QDs into a conventional immunoassay for the ultrasensitive detection of ochratoxin A (OTA) in food samples (Scheme 1). OTA is a common mycotoxin that has been categorized as a potential human group 2B carcinogen by the International Agency for Research on Cancer (IARC).[40] Fluorescent ELISA was performed using a mouse anti-OTA monoclonal antibody (mAb) and a catalase (CAT)–OTA conjugate as the

coating antibody and competitive antigen, respectively. CAT was used to accelerate the decomposition of H_2O_2 due to its excellent catalytic ability. In theory, one CAT molecule can convert approximately 40 000 000 molecules of H_2O_2 to water and oxygen per second,[41] which is about 240-fold higher than that of horseradish peroxidase (HRP, 10^7 molecules of substrate per minute[42]). Through the ingenious combination of the use of H_2O_2-induced fluorescence quenching of CdTe QDs as a fluorescent signal output and the ultrahigh catalytic activity of CAT to H_2O_2, the half maximal inhibitory concentration (IC_{50}) and the limit of detection (LOD) of our proposed method were 0.53 and 0.05 pg mL^{-1}, respectively. These values were approximately 283- and 300-folds lower than those of HRP-based conventional ELISA (0.15 ng mL^{-1} IC_{50} and 0.015 ng mL^{-1} LOD; Fig. S3, ESI†). The analytical performances of our developed method were evaluated on the basis of accuracy, precision, specificity, and practicability by using OTA-spiked agricultural products. The results demonstrated that our proposed fluorescent ELISA can be applied for the ultrasensitive detection of OTA molecules in actual food samples.

2. Materials and methods

2.1 Materials

N,*N*′-Dicyclohexylcarbodiimide (DCC), *N*-hydroxysuccinimide (NHS), bovine liver CAT, bovine serum albumin (BSA), protein G, and H_2O_2 were purchased from Sigma-Aldrich Chemical Co. (St. Louis, MO, USA). Mouse anti-OTA mAb was obtained from Jiangxi Zodolabs Biotech Corp. (Jiangxi, China) and MPA was obtained from Alfa Aesar. Tellurium powder, cadmium nitrate, and sodium borohydride were procured from the Institute of Tianjin Jinke Fine Chemicals. Other reagents were of analytical grade and purchased from Sinopharm Chemical Corp. (Shanghai, China). All chemicals and materials were used without further purifications. Furthermore, 96-well microplates (high binding and white or black) were obtained from Costar Inc. (Cambridge, MA, USA).

2.2 Synthesis of water-soluble CdTe QDs

The water-soluble CdTe QDs were synthesized according to a previously reported method.[31] In brief, a freshly prepared NaHTe solution was mixed with a nitrogen-saturated $Cd(NO_3)_2$ solution at pH 11.2 (adjusted by dropwise addition of 1 M NaOH) in the presence of MPA as a stabilizing agent; the final concentrations of NaHTe, $Cd(NO_3)_2$, and MPA were 0.76, 1.74, and 2.55 mg mL^{-1}, respectively. The CdTe precursor solution was heated in a water bath at 95 °C. Finally, the resulting CdTe QD solution was stored at 4 °C for future use. The photoluminescence spectrum of the CdTe QDs was recorded by using a fluorescence spectrophotometer (Hitachi F-4500, Tokyo, Japan), and the UV-vis absorption spectra of the CdTe QDs were obtained with an Amersham Pharmacia Ultrospec 4300 pro UV/visible spectrophotometer (England, UK). The size distribution and morphology of the prepared CdTe QDs were characterized by using a high-resolution transmission electron microscope (TEM, JEOL JEM 2100; Tokyo, Japan). The average hydrodynamic diameter and zeta-potential of the resulting CdTe QDs were determined with a particle size analyzer (Zeta Sizer Nano ZS90, Malvern Instruments Ltd, Worcestershire, UK). The fluorescence

†Electronic supplementary information (ESI) available. See DOI: 10.1039/c6nr01136e

quantum yield (QY) of the synthetic CdTe QDs was determined using rhodamine 6G as a reference standard (QY = 95%) according to a previously described method.[43,44]

2.3 Preparation of CAT–OTA conjugates

The CAT–OTA conjugates were synthesized through the formation of peptide bonds between the carboxyl group of OTA and the amino group of CAT in the presence of DCC/NHS, as previously described.[45] In brief, the carboxyl group of OTA was activated by suspending OTA, DCC, and NHS in 250 μL of DMF at a mole ratio of 1 : 5 : 5. After the mixture was stirred in the dark at room temperature for 2 h, the activated solution was centrifuged at 6700*g* for 15 min to remove excess DCC and then added into the CAT solution with OTA and CAT (mole ratio of 5 : 1). After the solution was stirred overnight in the dark at room temperature, the reaction solution was dialyzed against 0.01 M PBS (pH 7.4) for 72 h at 4 °C.

2.4 Procedure of direct competitive fluorescence ELISA for OTA

First, 96-well microplates were modified with 100 μL of protein G (20 μg mL^{-1}) in bicarbonate buffer (100 mM, pH 8.6) at 4 °C overnight. After the microplates were washed thrice with washing buffer (PBS, pH 7.4, 0.01 M, containing 0.05% Tween 20), the plates were blocked with blocking buffer (1 mg mL^{-1} of BSA in PBS) for 2 h at 37 °C. The plates were washed thrice with washing buffer, and 100 μL of anti-OTA mAb diluted to 1 : 3200 in PBS was added for 2 h at room temperature. After the plates were washed thrice with washing buffer, 50 μL per well of CAT–OTA conjugates was diluted to 1 : 1280 in 0.02 M PB (pH 7.0) with 5 mM NaCl. The solution was added and incubated in 50 μL per well of OTA standards to a desired final concentration ranging from 0 pg mL^{-1} to 100 pg mL^{-1} by diluting a stock solution with PB (0.02 M, pH 7.0) containing 5 mM NaCl and 5% methanol. After 30 min at 37 °C, the unbound content was discarded, and the microplates were washed thrice with washing buffer and twice with PBS. Then, 100 μL of 10 μM H_2O_2 in 0.01 M PBS (pH 7.4) per well was added to the microplates. After 30 min, 50 μL of freshly prepared CdTe QDs diluted to 1 : 400 in 0.01 M PBS (pH 7.4) was added to each well. After the QDs were incubated for 15 min, the fluorescence signals from the CdTe QDs were determined (excitation at 310 nm, emission at 590 nm) by using a microplate reader (Thermo Varioskan Flash, Thermo, USA). For comparison, a HRP-based conventional ELISA was developed, and the detailed procedures are provided in the ESI.†

2.5 Sample preparation

Corn, wheat, and rice samples collected from a local grocery store were finely ground and stored in a freezer at −20 °C before analysis was conducted. The samples for fluorescence ELISA were prepared in accordance with a previously reported method with some modifications. In brief, 1 g of a finely ground sample was weighed and spiked with 4, 10, 20, and 40 μg kg^{-1} OTA. The spiked samples were extracted with 5 mL of 50% (v/v) methanol in ultrapure water with vigorous shaking for 20 min. The mixture was centrifuged at 8000*g* for 20 min and the supernatant containing OTA was stored at 4 °C for fluorescence ELISA analysis.

3. Results and discussion

3.1 Characterization of H_2O_2-induced fluorescence quenching of CdTe QDs

The CdTe QDs were synthesized in an aqueous phase, following a previously described method.[31] The absorption and fluorescence spectra of the as-prepared CdTe QDs are presented in Fig. 1A. The UV-vis spectrum revealed that the CdTe QDs exhibit a maximum absorption peak at 570 nm; the fluorescence emission spectrum of the CdTe QDs showed a bright and narrow fluorescence emission peak at 590 nm. This result indicated that the CdTe QDs are monodispersed. The inset in Fig. 1A showed that the as-prepared CdTe QD aqueous solution was transparent red in color under natural light, but emitted an orange fluorescence under UV light (365 nm). The TEM images in Fig. 1B suggest that the CdTe QDs display a narrow size distribution with an average size of 4 ± 1 nm (n = 50). The inset in Fig. 1B revealed that the average hydrodynamic diameter of the resultant CdTe QDs was 4.02 ± 1.92 nm. Furthermore, the zeta-potential of the resultant CdTe QDs was −28.8 ± 1.52 mV. In addition, the QY of the resulting CdTe QDs could reach up to 67% and be stable at 4 °C for 12 months in the presence of MPA, which is in accordance with the previous reports.[46] On the basis of these results, we concluded that our CdTe QDs exhibit uniform size distribution and good optical properties.

The fluorescence quenching of the CdTe QDs by H_2O_2 was investigated by incubating CdTe QDs (12.5 nM) with different amounts of H_2O_2 (0–100 μM) at room temperature for 15 min in accordance with a previously reported method.[31–34] Fluorescence quenching efficiency was calculated by $(F_0 - F)/F_0 \times 100\%$, where F_0 and F represent the fluorescence intensities of CdTe QDs without and with the desired H_2O_2 concentrations, respectively. Fig. 1C indicates that the fluorescence quenching efficiency of the CdTe QDs increased sharply as the H_2O_2 concentration increased from 0 μM to 6.25 μM, and then plateaued when the H_2O_2 concentration was further increased to 10 μM. The inset in Fig. 1C shows that the change of fluorescence quenching of the CdTe QDs has a good relationship with the concentration of H_2O_2 ranging from 0 μM to 6.25 μM. The LOD of the CdTe QDs for H_2O_2 was calculated to be 0.136 μM, demonstrating that the fluorescence of the synthetic CdTe QDs was extremely sensitive to H_2O_2 concentration in solution. To obtain a stable fluorescence quenching signal, we designated 10 μM H_2O_2 as the optimal concentration in the subsequent experiments. Under the optimized concentration of H_2O_2, the fluorescence intensity of the QDs would be restored with the increased CAT concentration from 10^{-14} to 10^{-4} g mL^{-1} due to the decomposition of H_2O_2. The LOD of CAT to the restored fluorescent signal of CdTe QDs was calculated to be 10^{-14} g mL^{-1}, which was defined as the lowest concentration of CAT that generated a higher fluorescence intensity than blank fluorescence intensity plus 3 standard deviations (Fig. 1D), which was about 100-fold lower than that of HRP to tetramethylbenzidine (ESI, Fig. S1†). The above results indicate that an ultralow amount of CAT was able to cause significant changes in H_2O_2 concentration in order to generate remarkable fluorescence signal fluctuations, thereby generating the ultrahigh sensitivity of the fluorescent immunoassay. In addition, the effects of the incubation time of H_2O_2 and CdTe QDs on the fluorescence quenching of CdTe QDs were also investigated. Fig. S–2A and S–2B† show that the fluorescence-quenching efficiency of CdTe QDs increased as the incubation time was prolonged from 0 min to 13 min until a stable value

was reached. Thus, 15 min of incubation time between H_2O_2 and CdTe QDs was necessary to improve the reproducibility of fluorescence quenching.

3.2 Development of direct competitive fluorescence ELISA based on H_2O_2-induced fluorescence quenching of QDs

A schematic of H_2O_2-induced fluorescence quenching based competitive ELISA is presented in Scheme 1. When the OTA molecule was absent from the sample solution, the CAT–OTA conjugate (competitive antigen) was captured by the anti-OTA mAb pre-coated in the microplate. The fluorescence of CdTe QDs was not quenched because H_2O_2 was consumed by the CAT enzyme; as a result, a high fluorescence signal was detected. Conversely, the presence of OTA caused the target OTA to competitively bind to the anti-OTA mAb in the microplate; therefore, a low amount of CAT enzyme was detected in the microplate. More H_2O_2 led to a stronger fluorescence quenching of CdTe QDs, and a low fluorescence signal was obtained. Therefore, recording the change in fluorescence signals can facilitate the detection of analytes.

In direct competitive ELISA, the concentrations of coating antibody and competitive antigen are two key parameters that determine detection sensitivity. The concentrations of coating antibody and competitive antigen were optimized through checkerboard titration to achieve the highest sensitivity. The competitive inhibition rates and fluorescence intensities of the negative control were considered to confirm the optimum parameters. The competitive inhibition rates were obtained using the following equation: $(1 - F/F_0) \times 100\%$, where F_0 and F represent the fluorescence intensity of the negative control (OTA-free) and an OTA-spiked PBS solution (1 ng mL^{-1}), respectively. Table S1† shows that the optimum working concentrations are 3200-fold diluted in anti-OTA mAb (1 mg mL^{-1}) as a coating antibody and 1280-fold diluted in CAT–OTA conjugates (0.72 mg mL^{-1}) as a competitive antigen, respectively. Under the optimized combinations, the normalized fluorescence intensity of the negative control was 5.36 and the competitive inhibition rate of the fluorescence ELISA for 1 ng mL^{-1} OTA sample was achieved at 95.22%.

The change in pH and NaCl concentration could significantly influence the immunoreactions between the antigen and antibody by changing the activity of the antigen-combining sites of antibody molecules.[47] Thus, the effects of pH and NaCl concentration of the sample solution on the sensitivity of fluorescence ELISA were evaluated. Furthermore, the immunoreaction time between the anti-OTA antibody and OTA–CAT and the duration of the enzyme hydrolysis of H_2O_2 were optimized. The effects of pH on the sensitivity of fluorescence ELISA are shown in Fig. 2A. The fluorescence signal of the resultant ELISA was more likely influenced at pH 4.0 and 9.0 because the fluorescence intensity of the negative control was less than 1.0. When the pH ranged from 5.0 to 8.0, the fluorescence intensity of the negative control was greater than 6.35 ± 1.41; in contrast, IC_{50} varied in a narrow range from 0.71 pg mL^{-1} to 1.19 pg mL^{-1}. This finding showed that this immunoassay could be performed at a pH ranging from 5.0 to 8.0. Given the low IC_{50}, pH 7.0 was selected as the optimum pH for the subsequent experiments. To explore the effects of NaCl concentration on the sensitivity of fluorescence ELISA, a PB buffer (0.02 M, pH 7.0) containing 5, 10, 25, 50, 100 mM NaCl, and a PBS solution (0.01 M, pH 7.4) were used

to perform the fluorescence ELISA. Fig. 2B shows that the IC_{50} increased as the NaCl concentration increased from 5 mM to 100 mM, and the lowest IC_{50} was observed at 5 mM NaCl. The extract solution containing a certain concentration of methanol was required to obtain a higher extraction recovery from the actual OTA-polluted samples because of the strong hydrophobic property of OTA. However, the antigen–antibody interaction can be influenced by methanol;[48] as such, we investigated the effects of different methanol concentrations ranging from 0% to 25% on fluorescence immunoassay. In Fig. 2C, the lowest IC_{50} at 0.52 pg mL^{-1} was obtained when the methanol concentration was 5%. Considering the high sensitivity of the proposed method, we recommend that the actual sample extract should be diluted with 0.02 M PB (pH 7.0, 5 mM NaCl) to obtain a final methanol concentration of 5%. Hence, the PB buffer (0.02 M, pH 7.0) containing 5 mM NaCl and 5% methanol served as the optimal assay buffer in the subsequent experiments. Fig. 2D illustrates the effect of the time of immunoreaction between the anti-OTA antibody and OTA–CAT on the sensitivity of fluorescence ELISA. The fluorescence intensity of the negative control was considerably increased as immuno-reaction time was extended. The IC_{50} values decreased first and then increased as the immunoreaction time was extended from 15 min to 60 min. The lowest IC_{50} at 0.51 pg mL^{-1} was observed at 30 min. Thus, 30 min of immunoreaction time was necessary to enable the high sensitivity and reproducibility of the fluorescence ELISA. The effect of enzyme hydrolysis time on the detection sensitivity of immunoassay is shown in Fig. 2E. The results show that the fluorescence intensity increased greatly as the enzyme reaction time was extended, and the lowest IC_{50} at 0.53 pg mL^{-1} was observed when the enzyme reaction time was 30 min.

3.3 Analytical performance of the fluorescence ELISA

Under the optimized conditions, a direct competitive fluorescence ELISA standard curve was established. The $F/F_0 \times 100\%$ was plotted against the logarithm of various concentrations of the OTA standard solution (0–100 pg mL^{-1}), where F_0 and F represent the normalized fluorescence intensity of the negative control and an OTA standard solution, respectively. Fig. 3 shows that the calibration curve of the developed fluorescence ELISA exhibited a good linear range from 0.05 pg mL^{-1} to 10 pg mL^{-1} with a reliable correlation coefficient ($R^2 = 0.9948$). The regression equation is represented by $y = -17.2435 \ln(x) + 38.9783$, where y is the $F/F_0 \times 100\%$ and x is the OTA concentration. Error bars were based on three duplicate measurements at different OTA concentrations. The IC_{50} of the fluorescence ELISA was achieved at 0.53 pg mL^{-1}, which is 283-fold lower than that of conventional HRP-based ELISA (IC_{50} = 0.15 ng mL^{-1}; Fig. S3, ESI†). Moreover, the LOD, defined as IC_{10},[49] was calculated to be 0.05 pg mL^{-1}, which is comparable to those of other methods developed recently for the detection of OTA (Table S2†). The ultrahigh sensitivity caused by the fluorescence of CdTe QDs was extremely sensitive to the ultralow concentration of H_2O_2 in solution, and the ultrahigh catalytic activity of CAT to H_2O_2.

To determine the specificity of the developed assay, we performed fluorescence ELISA using three common mycotoxins and their mixtures, including OTA (0.5 pg mL^{-1}), aflatoxin B_1 (AFB_1, 1 ng mL^{-1}), and zearalenone (ZEN, 1 ng mL^{-1}). A negative control test was performed by adding a PB (0.02 M, pH 7) solution containing 5 mM NaCl and 5% methanol. Fig. 4 shows that significant decreases of $F/F_0 \times 100\%$ were only observed in

these sample solutions with OTA. Negligible changes were observed in these sample solutions without OTA compared with the negative control, indicating the excellent selectivity of the proposed fluorescence ELISA for OTA.

The precision of the intra-assay and inter-assay variations was used to evaluate the accuracy of the developed fluorescence ELISA. The intra-assay was performed in triplicate on the same day, and the inter-assay was carried out on six consecutive days. Recovery studies for the intra-assay and interassay were conducted by analyzing three samples spiked with four different concentrations of OTA (4, 10, 20, and 40 μg kg^{-1}). Table 1 shows the average recoveries for intra-assay ranging from 86.28% to 102.30%, with the coefficient of variation (CV) ranging from 4.96% to 17.67%. The average recoveries for the inter-assay ranged from 90.90% to 104.75%, and the CV ranged from 5.69% to 18.36%. The variations in intra-assay and inter-assay using fluorescence ELISA exhibit acceptable levels of precision for the quantitative analysis of OTA.[47]

3.4 Assay validation

To evaluate the acceptability of the new fluorescence ELISA for OTA, a comparative study with a conventional ELISA method was performed through addition and recovery tests. Three kinds of food samples (OTA-free) including rice, wheat, and corn were spiked with known concentrations of OTA (Table 2). All samples were simultaneously analyzed with conventional ELISA and our proposed method. The results in Table 2 show that the average recovery of our proposed method ranged from 87.75% to 116.75%, with a CV ranging from 4.50% to 15.05%. Meanwhile, the average recovery of conventional ELISA ranged from 82.2% to 121.25%, with a CV ranging from 5.82% to 17.44%. The above results indicate that the newly developed fluorescence ELISA is comparable with conventional ELISA and no significant difference in the quantitative determination of OTA was observed between the two methods ($p > 0.05$). In addition, these results show that fluorescence ELISA can be used to detect ultralow concentrations of OTA in actual food samples. The ultrahigh sensitivity of our method allows the repeated dilution of complex food samples, thus largely eliminating the background matrix interference.

4. Conclusions

In the present study, H_2O_2-induced fluorescence quenching of CdTe QDs was introduced along with conventional ELISA for the first time. The developed fluorescent ELISA could ultra-sensitively detect OTA through the integration of two signal-amplification factors, including H_2O_2-induced fluorescence quenching of CdTe QDs as a fluorescent signal output and a high catalytic activity of CAT to H_2O_2. Under the optimum conditions, the developed approach exhibited the dynamic linear detection of OTA from 0.05 pg mL^{-1} to 10 pg mL^{-1}. IC_{50} was 0.53 pg mL^{-1} and LOD was 0.05 pg mL^{-1}, which were about 283- and 300-folds lower than those of HRP-based conventional ELISA, respectively. The proposed method also exhibited good accuracy, high reproducibility, and excellent specificity against other mycotoxins in agricultural products. Therefore, fluorescent immunoassays based on the described H_2O_2-induced fluorescence quenching of CdTe QDs could serve as a potential

platform for the rapid and highly sensitive detection of mycotoxins or haptens in food safety monitoring.

Supplementary Material

Refer to Web version on PubMed Central for supplementary material.

Acknowledgments

This work was supported in part by the National Basic Research Program of China (2013CB127804), the Training Plan for the Main Subject of Academic Leaders of Jiangxi Province (20142BCB22004), the Training Plan for the Young Scientist (Jinggang Star) of Jiangxi Province (20142BCB23004), the Innovation Fund Designated for Graduate Students of Nanchang University (cx2015107), and the Intramural Research Program, National Institute of Biomedical Imaging and Bioengineering, National Institutes of Health.

References

1. Chen F, Hou S, Li Q, Fan H, Fan R, Xu Z, Zhala G, Mai X, Chen X, Chen X. Anal. Chem. 2014; 86:10021–10024. [PubMed: 24517078]
2. Liu D, Yang J, Wang H-F, Wang Z, Huang X, Wang Z, Niu G, Hight Walker A, Chen X. Anal. Chem. 2014; 86:5800–5806. [PubMed: 24896231]
3. Qu Z, Xu H, Xu P, Chen K, Mu R, Fu J, Gu H. Anal. Chem. 2014; 86:9367–9371. [PubMed: 25196700]
4. Xianyu Y, Chen Y, Jiang X. Anal. Chem. 2015; 87:10688–10692. [PubMed: 26460152]
5. Avrameas S. J. Immunol. Methods. 1992; 150:23–32. [PubMed: 1613256]
6. Nerurkar LS, Namba M, Brashears G, Jacob AJ, Lee YJ, Sever J. J. Clin. Microbiol. 1984; 20:109–114. [PubMed: 6086705]
7. Gould E, Buckley A, Cammack N. J. Virol. Methods. 1985; 11:41–48. [PubMed: 3891767]
8. De La Rica R, Stevens MM. Nat. Protoc. 2013; 8:1759–1764. [PubMed: 23975259]
9. Song Y, Xia X, Wu X, Wang P, Qin L. Angew. Chem., Int. Ed. 2014; 126:12659–12663.
10. Liu D, Huang X, Wang Z, Jin A, Sun X, Zhu L, Wang F, Ma Y, Niu G, Hight Walker AR. ACS Nano. 2013; 7:5568–5576. [PubMed: 23683064]
11. Surugiu I, Svitel J, Ye L, Haupt K, Danielsson B. Anal. Chem. 2001; 73:4388–4392. [PubMed: 11569836]
12. Glavan AC, Christodouleas DC, Mosadegh B, Yu HD, Smith BS, Lessing J, Fernández-Abedul MT, Whitesides GM. Anal. Chem. 2014; 86:11999–12007. [PubMed: 25470031]
13. Zhang Y, Yang J, Nie J, Yang J, Gao D, Zhang L, Li J. Chem. Commun. 2016; 52:3474–3477.
14. Xiang Y, Lan T, Lu Y. J. Diabetes Sci. Technol. 2014; 8:855–858. [PubMed: 25562889]
15. Song Y, Zhang Y, Bernard PE, Reuben JM, Ueno NT, Arlinghaus RB, Zu Y, Qin L. Nat. Commun. 2012; 3:1283. [PubMed: 23250413]
16. Guarrotxena N, Liu B, Fabris L, Bazan GC. Adv. Mater. 2010; 22:4954–4958. [PubMed: 20812231]
17. Rissin DM, Kan CW, Campbell TG, Howes SC, Fournier DR, Song L, Piech T, Patel PP, Chang L, Rivnak AJ. Nat. Biotechnol. 2010; 28:595–599. [PubMed: 20495550]
18. De La Rica R, Stevens MM. Nat. Nanotechnol. 2012; 7:821–824. [PubMed: 23103935]
19. Torrance L, Jones R. Ann. Appl. Biol. 1982; 101:501–509.
20. Frangioni JV. Curr. Opin. Chem. Biol. 2003; 7:626–634. [PubMed: 14580568]
21. Fang X, Tan W. Anal. Chem. 1999; 71:3101–3105. [PubMed: 21662902]
22. Lian W, Litherland SA, Badrane H, Tan W, Wu D, Baker HV, Gulig PA, Lim DV, Jin S. Anal. Biochem. 2004; 334:135–144. [PubMed: 15464962]
23. Ding S, Chen J, Jiang H, He J, Shi W, Zhao W, Shen J. J. Agric. Food Chem. 2006; 54:6139–6142. [PubMed: 16910698]

24. Wu Y, Wei P, Pengpumkiat S, Schumacher EA, Remcho VT. Anal. Chem. 2015; 87:8510–8516. [PubMed: 26186018]
25. Ren M, Xu H, Huang X, Kuang M, Xiong Y, Xu H, Xu Y, Chen H, Wang A. ACS Appl. Mater. Interfaces. 2014; 6:14215–14222. [PubMed: 25109633]
26. Resch-Genger U, Grabolle M, Cavaliere-Jaricot S, Nitschke R, Nann T. Nat. Methods. 2008; 5:763–775. [PubMed: 18756197]
27. Zhu X, Chen L, Shen P, Jia J, Zhang D, Yang L. J. Agric. Food Chem. 2011; 59:2184–2189. [PubMed: 21329353]
28. Zhang Z, Li Y, Li P, Zhang Q, Zhang W, Hu X, Ding X. Food Chem. 2014; 146:314–319. [PubMed: 24176348]
29. Lin P-C, Chen S-H, Wang K-Y, Chen M-L, Adak AK, Hwu J-RR, Chen Y-J, Lin C-C. Anal. Chem. 2009; 81:8774–8782. [PubMed: 19874051]
30. Pathak S, Davidson MC, Silva GA. Nano Lett. 2007; 7:1839–1845. [PubMed: 17536868]
31. Meng X, Wei J, Ren X, Ren J, Tang F. Biosens. Bioelectron. 2013; 47:402–407. [PubMed: 23612061]
32. Shiang Y-C, Huang C-C, Chang H-T. Chem. Commun. 2009:3437–3439.
33. Dasog M, Scott RW. Langmuir. 2007; 23:3381–3387. [PubMed: 17269805]
34. Chen Z, Ren X, Meng X, Zhang Y, Chen D, Tang F. Anal. Chem. 2012; 84:4077–4082. [PubMed: 22486298]
35. Yang L, Ren X, Meng X, Li H, Tang F. Biosens. Bioelectron. 2011; 26:3488–3493. [PubMed: 21376562]
36. Chen Z, Ren X, Meng X, Chen D, Yan C, Ren J, Yuan Y, Tang F. Biosens. Bioelectron. 2011; 28:50–55. [PubMed: 21816604]
37. Azmi NE, Ramli NI, Abdullah J, Hamid MAA, Sidek H, Rahman SA, Ariffin N, Yusof NA. Biosens. Bioelectron. 2015; 67:129–133. [PubMed: 25113659]
38. Jin D, Seo M-H, Huy BT, Pham Q-T, Conte ML, Thangadurai D, Lee Y-I. Biosens. Bioelectron. 2016; 77:359–365. [PubMed: 26433069]
39. Guo C, Wang J, Cheng J, Dai Z. Biosens. Bioelectron. 2012; 36:69–74. [PubMed: 22521943]
40. Rivas L, Mayorga-Martínez CC, Quesada-González D, Zamora A, de la Escosura-Muñiz A, Merkoçi A. Anal. Chem. 2015; 87:5167–5172. [PubMed: 25901535]
41. Gao Z, Xu M, Hou L, Chen G, Tang D. Anal. Chem. 2013; 85:6945–6952. [PubMed: 23806145]
42. Zhang B, Tang D, Goryacheva IY, Niessner R, Knopp D. Chem. Eur. J. 2013; 19:2496–2503. [PubMed: 23292875]
43. Fery-Forgues S, Lavabre D. J. Chem. Educ. 1999; 76:1260–1264.
44. Idowu M, Lamprecht E, Nyokong T. J. Photochem. Photobiol., A. 2008; 198:7–12.
45. Kawamura O, Sato S, Kajii H, Nagayama S, Ohtani K, Chiba J, Ueno Y. Toxicon. 1989; 27:887–897. [PubMed: 2781587]
46. Weng J, Song X, Li L, Qian H, Chen K, Xu X, Cao C, Ren J. Talanta. 2006; 70:397–402. [PubMed: 18970782]
47. Huang X, Aguilar ZP, Li H, Lai W, Wei H, Xu H, Xiong Y. Anal. Chem. 2013; 85:5120–5128. [PubMed: 23614687]
48. Liu X, Xu Y, Wan D-B, Xiong Y-H, He Z-Y, Wang X-X, Gee SJ, Ryu D, Hammock BD. Anal. Chem. 2015; 87:1387–1394. [PubMed: 25531426]
49. Wang Y, Ning B, Peng Y, Bai J, Liu M, Fan X, Sun Z, Lv Z, Zhou C, Gao Z. Biosens. Bioelectron. 2013; 41:391–396. [PubMed: 23017676]

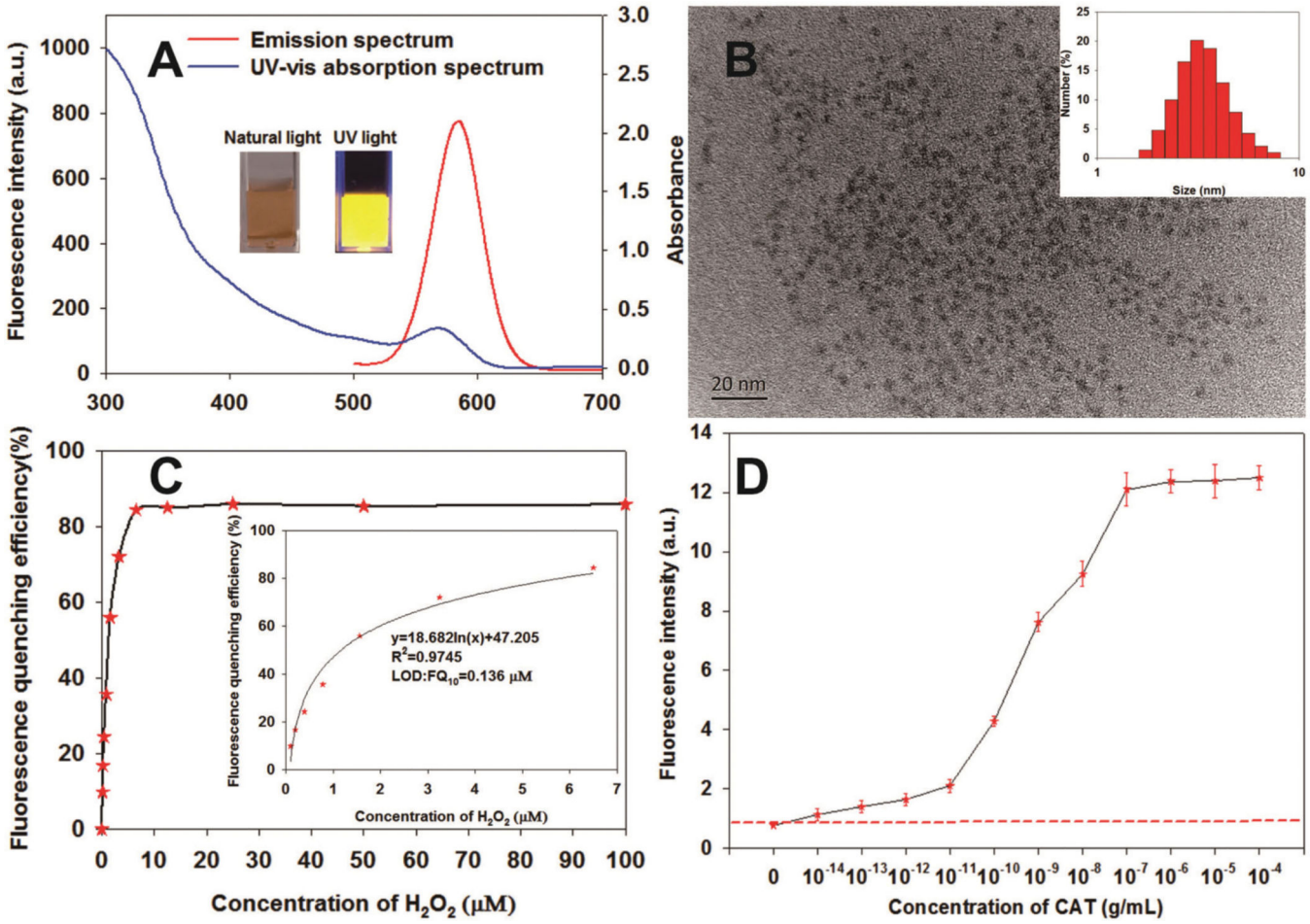

Fig. 1.

(A) Photoluminescence and UV-vis absorption spectra of CdTe QDs; the insets in (A) are the photographs of the CdTe QD solution under natural light (left) and UV light (365 nm) (right). (B) TEM image of the CdTe QD; the insets in (B) are the size distribution histograms of the CdTe QD. (C) Fluorescence changes upon the interaction of CdTe QD with different concentrations of H_2O_2 ranging from 0 to 100 μM. (D) Fluorescence changes upon the interaction of CdTe QD with different concentrations of CAT ranging from 0 to 10^{-4} g mL^{-1} in the presence of 10 μM H_2O_2. The red dashed line represents the blank fluorescence intensity plus 3 standard deviations. Thus, the LOD of CAT to the CdTe QDs was calculated as 10^{-14} g mL^{-1}, which was defined as the lowest concentration of CAT that generated a higher fluorescence intensity than blank fluorescence intensity plus 3 standard deviations.

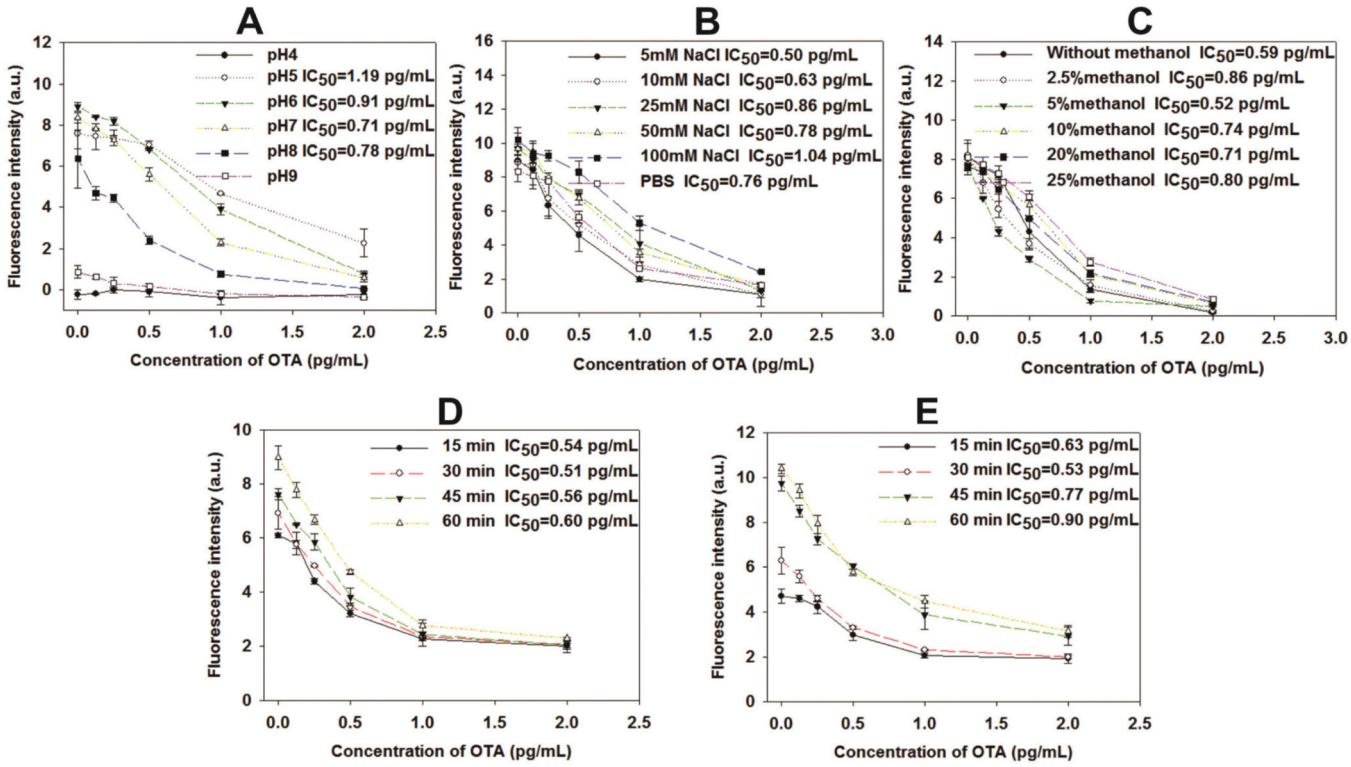

Fig. 2.

Optimization of the experimental conditions for fluorescence ELISA. The effects of (A) pH, (B) NaCl concentration, (C) methanol concentration, (D) immunoreaction time, and (E) enzyme reaction time on the performance of the direct competitive immunoassay. Vertical bars indicate the standard deviation ($n = 3$).

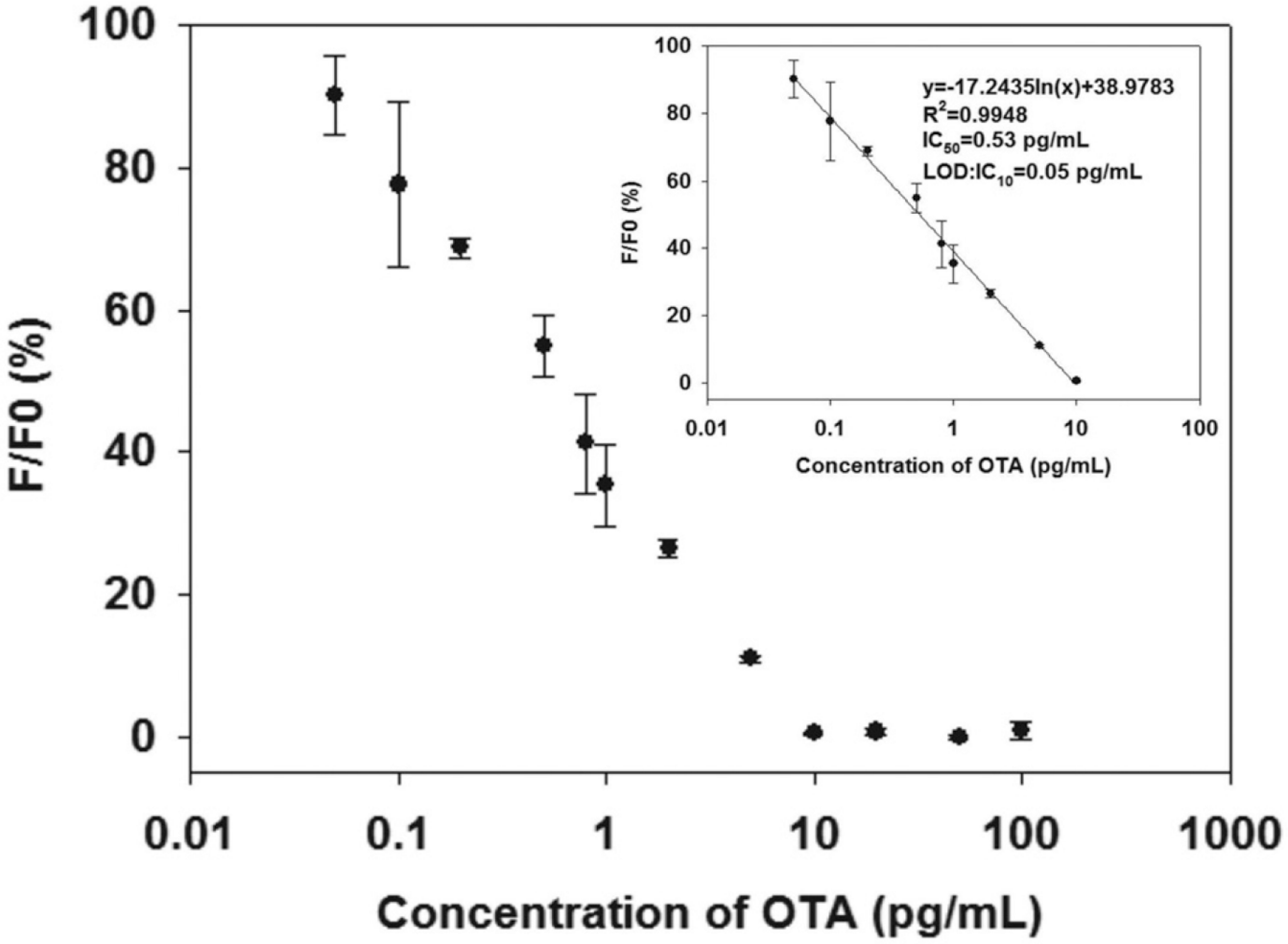

Fig. 3.

Quantitative immunoassay of OTA by using the developed fluorescent ELISA in spiked PB solution (0.02 M, pH 7) containing 5 mM NaCl and 5% methanol with OTA concentrations ranging from 0 pg mL^{-1} to 100 pg mL^{-1}. Vertical bars indicate the standard deviation (n = 3).

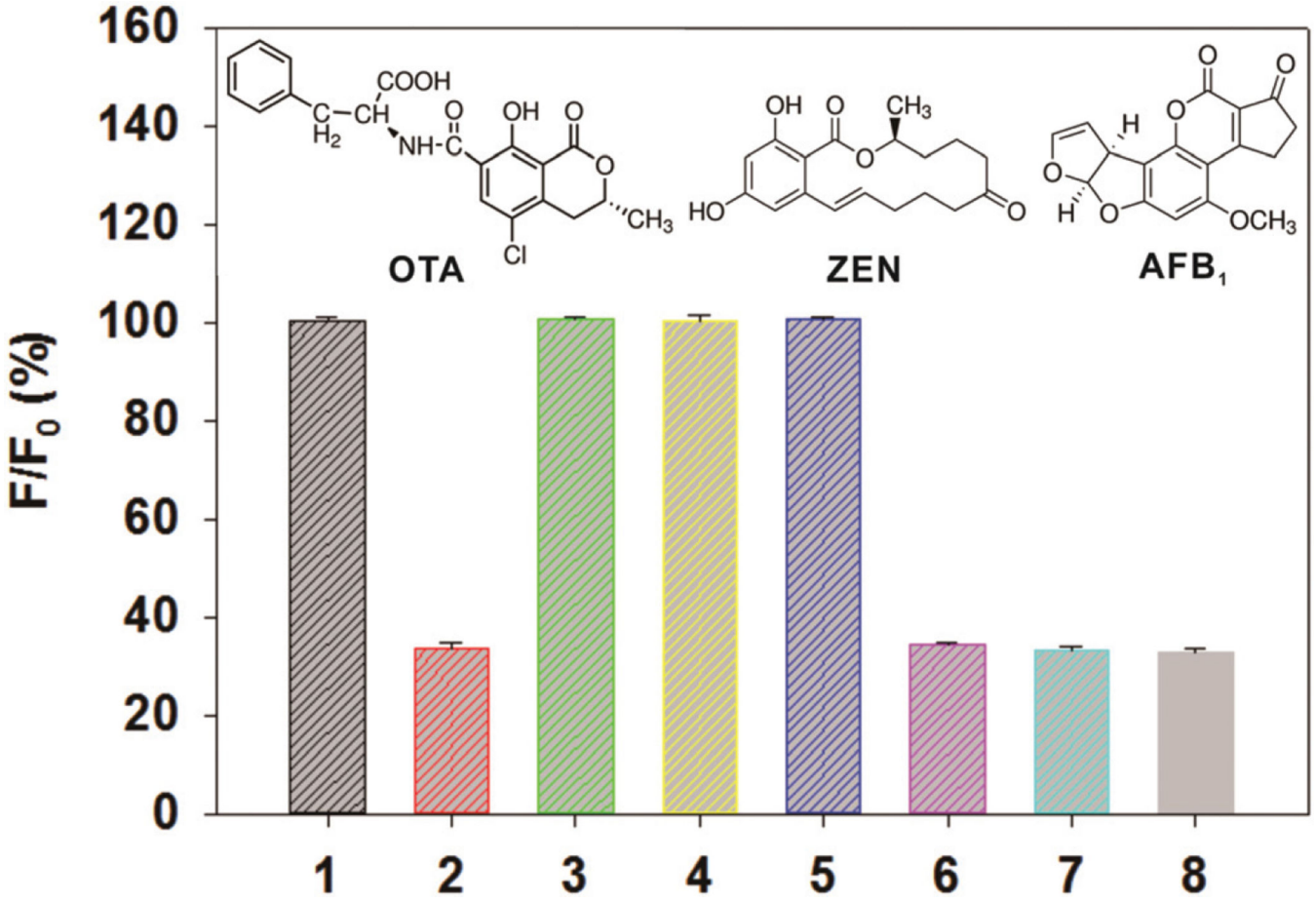

Fig. 4.

Specificity experiment for OTA, ZEN, and AFB_1. 1: control. 2: OTA (0.5 pg mL^{-1}). 3: AFB_1 (1 ng mL^{-1}). 4: ZEN (1 ng mL^{-1}). 5: AFB_1 (1 ng mL^{-1}) + ZEN (1 ng mL^{-1}). 6: AFB_1 (1 ng mL^{-1}) + OTA (0.5 pg mL^{-1}). 7: ZEN (1 ng mL^{-1}) + OTA (0.5 pg mL^{-1}). 8: AFB_1 (1 ng mL^{-1}) + ZEN (1 ng mL^{-1}) + OTA (0.5 pg mL^{-1}). Vertical bars indicate the standard deviation (n = 3). A negative control test was performed by adding the PB (0.02 M, pH 7) solution containing 5 mM NaCl and 5% methanol.

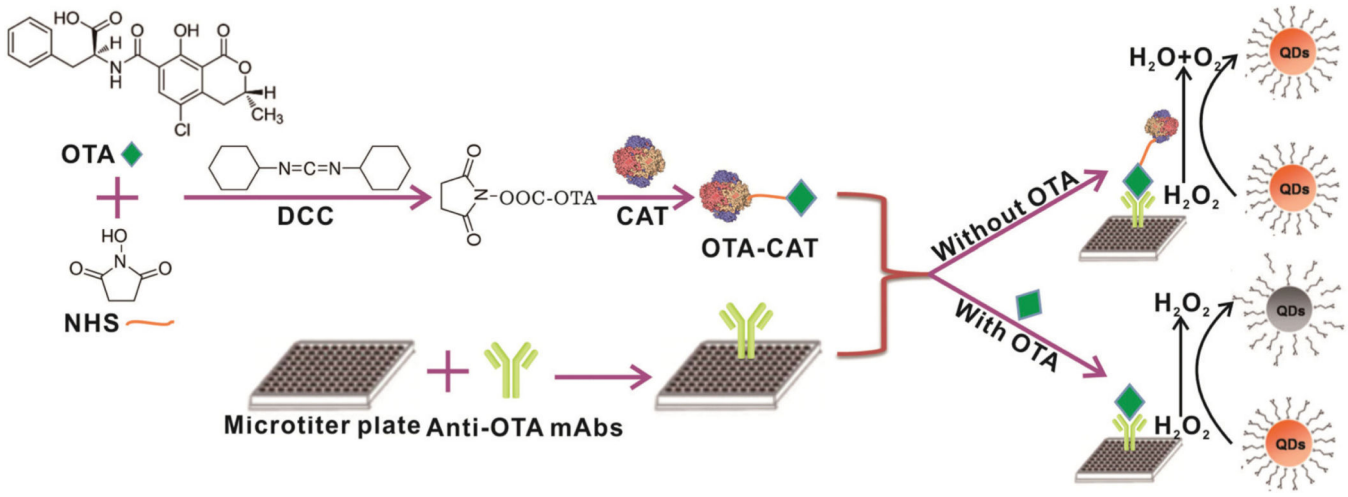

Scheme 1.
Schematic of the detection of OTA by using the proposed fluorescence ELISA.

Table 1

Precision assay of the proposed fluorescent ELISA

Sample matrix	OTA added (μg kg^{-1})	OTA recovered (μg kg^{-1})	Recovery (%)	CV (%)
Intra-assay (n = 3)[a]				
Wheat	4	3.92 ± 0.29	98.00	7.44
	10	10.22 ± 1.81	102.20	17.67
	20	18.75 ± 1.05	93.75	5.58
	40	40.54 ± 3.07	101.35	7.58
Corn	4	4.09 ± 0.63	102.25	15.35
	10	10.23 ± 0.85	102.30	8.30
	20	19.26 ± 3.00	96.30	15.58
	40	37.50 ± 2.70	93.75	7.21
Rice	4	3.48 ± 0.27	87.00	7.70
	10	9.12 ± 1.20	91.20	13.12
	20	17.72 ± 0.88	88.60	4.96
	40	34.51 ± 2.55	86.28	7.40
Inter-assay (n = 6)[b]				
Wheat	4	4.11 ± 0.43	102.75	10.49
	10	9.56 ± 1.48	95.60	15.53
	20	18.94 ± 1.08	94.70	5.69
	40	41.09 ± 2.72	102.73	6.61
Corn	4	4.19 ± 0.43	104.75	10.32
	10	9.79 ± 1.06	97.90	10.86
	20	19.21 ± 2.23	96.05	11.58
	40	38.83 ± 2.45	97.08	6.30
Rice	4	3.89 ± 0.71	97.25	18.36
	10	9.09 ± 0.92	90.90	10.09
	20	18.62 ± 1.77	93.10	9.51
	40	36.57 ± 3.37	91.43	9.21

[a]The assay was performed in three replicates on the same day.

[b]The assays were carried out on six consecutive days.

Table 2

Recoveries of OTA spiked to three food samples, including rice, wheat, and corn detected by fluorescent ELISA and conventional ELISA

	Fluorescent ELISA (n = 3)		Conventional ELISA (n = 3)	
OTA added (μg kg^{-1})	**OTA recovered (μg kg^{-1})**	**CV (%)**	**OTA recovered (μg kg^{-1})**	**CV (%)**
Wheat				
4	4.22 ± 0.24	5.75	3.91 ± 0.49	12.61
10	10.25 ± 0.55	5.37	10.35 ± 1.30	12.57
20	21.28 ± 1.84	8.65	21.57 ± 3.52	16.33
40	41.09 ± 5.51	13.40	39.48 ± 2.30	5.82
Corn				
4	3.51 ± 0.53	15.05	4.85 ± 0.84	17.44
10	9.76 ± 1.30	13.32	11.81 ± 1.60	13.51
20	21.26 ± 2.75	12.91	21.57 ± 1.32	6.13
40	41.64 ± 4.33	10.39	41.74 ± 6.38	15.29
Rice				
4	4.67 ± 0.48	10.28	4.64 ± 0.58	12.55
10	8.91 ± 0.85	9.52	8.22 ± 1.25	15.22
20	20.51 ± 0.92	4.50	19.88 ± 3.36	16.92
40	38.39 ± 2.29	5.96	39.99 ± 3.371	9.28